Biochemical Pharmacology 79 (2010) 825–841

Contents lists available at ScienceDirect

Biochemical Pharmacology

journal homepage: www.elsevier.com/locate/biochempharm

2-Methoxyestradiol induces endoreduplication through the induction of mitochondrial oxidative stress and the activation of MAPK signaling pathways

C.M. Ting [a], Y.M. Lee [a], C.K.C. Wong [a], A.S. Wong [b], H.L. Lung [c], M.L. Lung [c], K.W. Lo [d], R.N.S. Wong [a], N.K. Mak [a,*]

[a] Department of Biology, Hong Kong Baptist University, 224, Waterloo Road, Hong Kong
[b] School of Biological Sciences, University of Hong Kong, Hong Kong
[c] Department of Clinical Oncology, University of Hong Kong, Hong Kong
[d] Department of Anatomical and Cellular Pathology and State Key Laboratory in Oncology in South China, The Chinese University of Hong Kong, Hong Kong

ARTICLE INFO

Article history:
Received 1 September 2009
Accepted 21 October 2009

Keywords:
2-Methoxyestradiol
Endoreduplication
Oxidative stress
Nasopharyngeal carcinoma
MAPK signaling pathways
Mitochondria

ABSTRACT

2-Methoxyestradiol (2ME2) is a normal physiological metabolite of 17β-estradiol with anti-proliferative and anti-angiogenic activities. The purpose of this study is to elucidate the mechanism whereby 2ME2 induces endoreduplication of the well-differentiated nasopharyngeal carcinoma (NPC) cells. We report here that 2ME2 induces G2/M phase cell cycle arrest followed by endoreduplication of the well-differentiated HK-1 cells. The increase in chromosome number was confirmed by cytogenetic study. Analysis of stress signaling pathways revealed the phosphorylation activation of ERK, JNK and p38 MAPKs at various times after 2ME2 treatment. Pre-treatment of 2ME2-treated HK-1 cells with JNK inhibitor (SP600125), ERK inhibitor (PD98059) and p38 MAPK inhibitor (SB203580) resulted in the reduction of endoreduplicating cells. Furthermore, the increase in the phosphorylation of JNK was accompanied by an increase in the reactive oxygen species. In addition, endoreduplication was observed in cells after treatment with superoxide donor, 2,3-dimethoxy-1,4-naphoquinone (DMNQ). Confocal microscopic analysis also revealed the increase in mitochondrial superoxide anion in 2ME2-treated HK-1 cells. Pre-treatment of HK-1 cells with superoxide dismutase mimetic 2,2,6,6-tetramethylpiperidine-1-oxyl (TEMPO) or overexpressing the mitochondrial enzyme MnSOD resulted in the reduction of phosphorylation of JNK and the formation of endoreduplicating cells. Furthermore, the tubulin filaments in cytoplasm remain intact in 2ME2-treated HK-1 cells after pre-treatment of TEMPO. Our results suggest that 2ME2 induces endoreduplication through the induction of oxidative stress and the activation of MAPK signal pathways. The biological significance of drug-induced endoreduplication will also be discussed.

1. Introduction

2-Methoxyestradiol (2ME2) is a metabolite of endogenous estrogen 17β-estradiol (E_2). Recent studies showed that 2ME2 exerts both anti-tumour and anti-angiogenic activities on various tumours, and 2ME2 is now undergoing phase II clinical trial for cancer treatment [1]. The anti-tumour mechanism of 2ME2 is multi-faceted [2]. These included the induction of G1 or G2/M cell cycle arrest and tumour cell apoptosis [3–9]. Recent studies also indicated that 2ME2 induces G2/M arrest and interrupts the cell cycle progression via the binding to β-tubulin near the colchicine-binding site and the inhibition of microtubule polymerization [10,11].

Endoreduplication refers to the situation where DNA replication occurs without cell division [12]. Cells may undergo endoreduplication and become tetraploid or polyploid when the cells are arrested by the spindle assembly checkpoint or when the cells fail to undergo cytokinesis. Chemical compounds such as microtubule-interfering agents nocodazole and taxol had been shown to induce endoreduplication through the interruption of the segregation of sister chromatid [13,14]. Although 2ME2 is also considered as a microtubule-interfering agent, the mechanism of induction of endoreduplication in malignant cells has not been studied.

Reactive oxygen species (ROS), such as hydroxyl radicals, hydrogen peroxide and superoxide, are normally and constantly generated within a cellular environment [15]. Under normal conditions, ROS is known to mediate a wide variety of cellular responses including cell growth and differentiation. Prolonged and excessive production of ROS, and hence oxidative stress, may lead

* Corresponding author. Tel.: +852 34117059.
E-mail address: nkmak@hkbu.edu.hk (N.K. Mak).

0006-2952/$ – see front matter © 2009 Elsevier Inc. All rights reserved.
doi:10.1016/j.bcp.2009.10.018

to cell cycle arrest and cell death [16–18]. A previous study indicated that phenylhydroquinone-derived ROS may induce the endoreduplication of CHO-K1 ovarian cells [19]. However, the role of oxidative stress in 2ME2-induced endoreduplication is unknown. The present study aims to elucidate the role of oxidative stress in 2ME2-induced endoreduplication of human nasopharyngeal carcinoma cells. Results from this study indicated that 2ME2 induced G2/M arrest, followed by endoreduplication in HK-1 NPC cells. We further demonstrated that 2ME2 induced endoreduplication through the generation of mitochondrial oxidative stress and the subsequent activation of JNK.

2. Materials and methods

2.1. Chemicals

A stock solution of 20 mM of 2ME2 (Sigma Chemical Co.) was prepared by dissolving 2ME2 in DMSO. The stock solution was kept at −20 °C until use. Superoxide dismutase (SOD) mimetic 2,2,6,6-tetramethylpiperidine-1-oxyl (TEMPO), superoxide anion donor 2,3-dimethoxy-1,4-naphoquinone (DMNQ) and 4,6-diamidino-2-phenylindole (DAPI) were obtained from Sigma Chemical Co. Antibodies to phospho-JNKs, JNKs, phospho-p38 MAPKs, p38

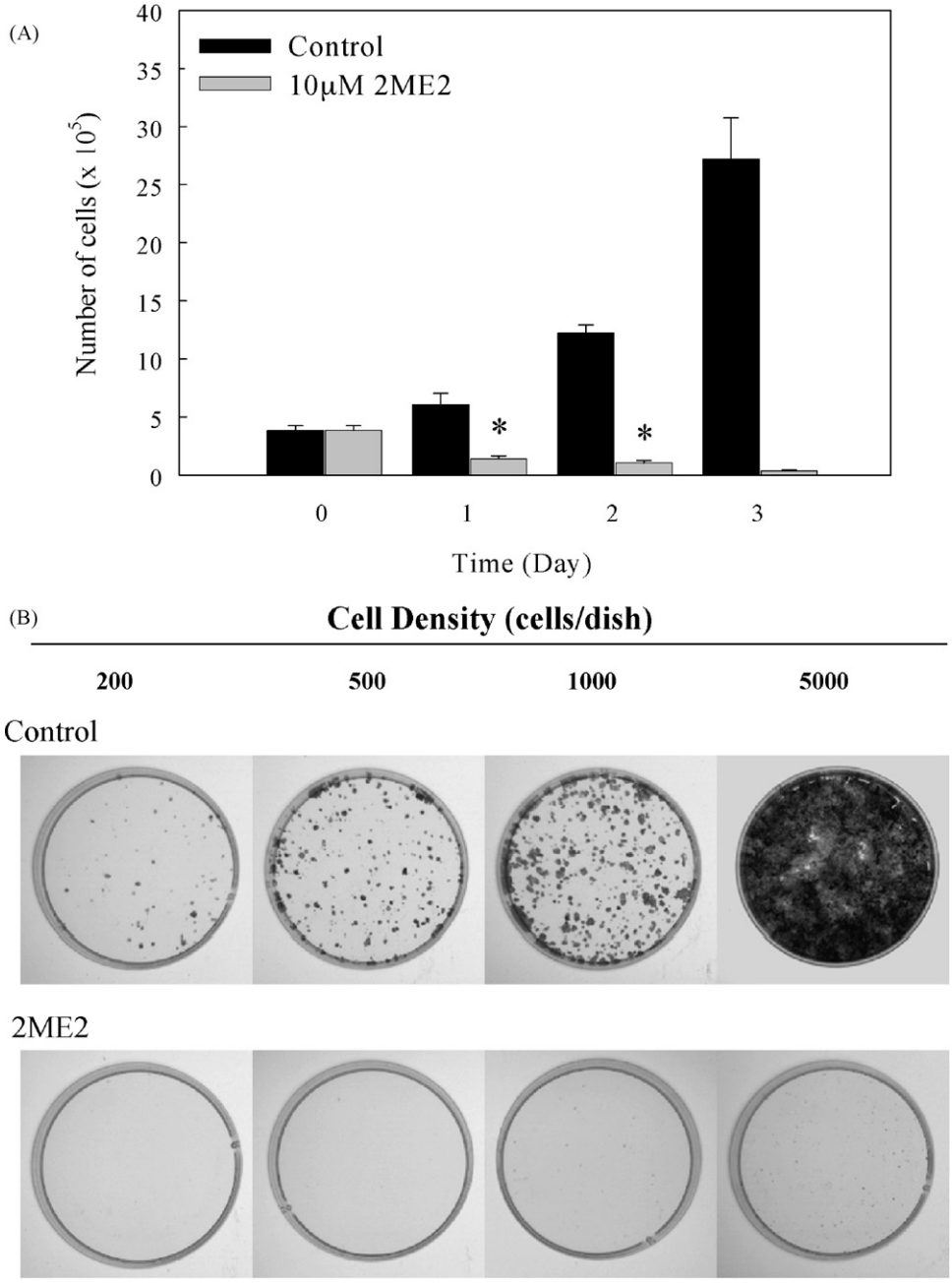

Fig. 1. 2ME2-induced growth inhibition of HK-1 cells. (A) Kinetics of growth inhibition. HK-1 cells (2×10^5 cells/dish) were seeded overnight and treated with 10 μM 2ME2. The number of viable HK-1 cells was determined by trypan blue exclusion assay at days 1, 2 and 3 after 2ME2 treatment. Results were expressed as mean ± SD of triplicates. Student's *t*-tests were performed for determination of the significant difference, $^*p < 0.05$. (B) Cologenicity of 2ME2-treated HK-1 cells. HK-1 cells (200–5000 cells/dish) were incubated with 2ME2 for 48 h. The cells were washed and further incubated in fresh medium for 7 days. The cells were then fixed and stained for the microscopic examination of colony formation as described in Section 2. (C) Physical characteristics of 2ME2-treated HK-1 cells. Upper panel: DIC images of 2ME2-treated HK-1 cells. Scale bar: 20 μm. Lower panel: flow cytometric analysis of 2ME2-treated HK-1 cells. Cell size was detected by the forward scatter (FSC) detector and the cell granularity was detected by the side scatter (SSC) detector. (D) Total chromosome number analysis of 2ME2-treated HK-1 cells. Chromosomes in the metaphase spreads stained with DAPI were counted. A total of 20 metaphases were counted for each treatment. Chromosome count: untreated HK-1, 64; 2ME2 (24 and 48 h), 128.

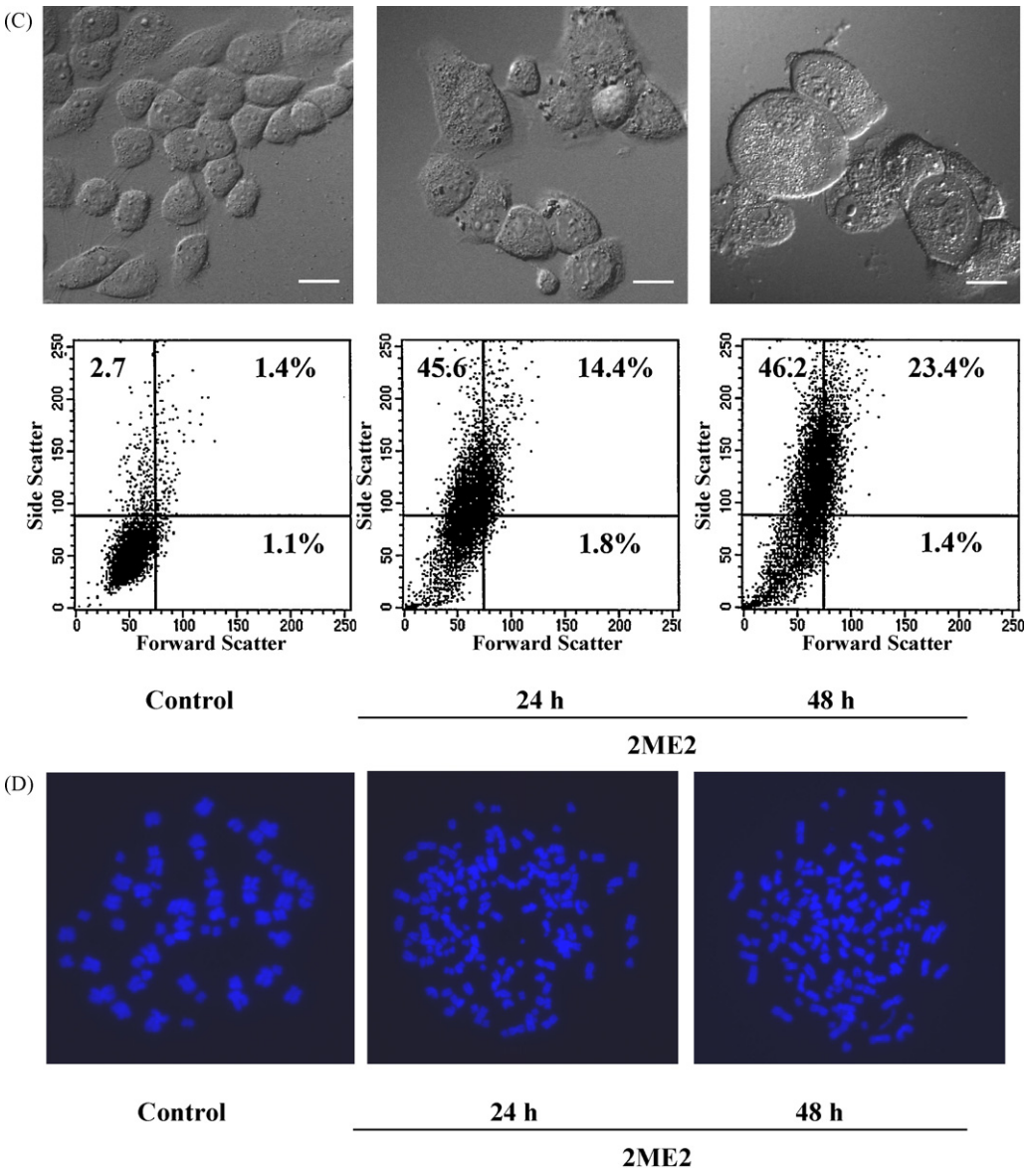

Fig. 1. (*Continued*).

MAPKs, phospho-ERKs and ERKs were purchased from Cell Signaling. Antibodies to β-tubulin and manganese superoxide dismutase (MnSOD) were obtained from Sigma Chemical Co. and Santa Cruz, respectively. Chemical inhibitors SP600125, SB203580 and PD98059 were obtained from Calbiochem (La Jolla, CA). MitoSOX™ Red mitochondrial superoxide indicator was purchased from Molecular Probes-Invitrogen (Eugene, OR).

2.2. Cell lines and cell culture

The well-differentiated HK-1 [20], EBV HK-1 [21] and C666-1 [22] cells were routinely maintained as monolayers in 25-cm^2 culture flask in RPMI-1640 supplemented with 10% fetal calf serum (FCS, Gibco) and antibiotics PS (50 μg/ml penicillin, 50 μg/ml streptomycin, Gibco). Cells were cultured at 37 °C in a humidified incubator (5% CO_2) and the cells were subcultured every 3–4 days.

2.3. Colony formation assay

Various numbers of HK-1 cells (200–5000 cells/dish) were seeded onto the 35 mm tissue culture dishes overnight. Cells were then incubated with 10 μM 2ME2 for 48 h. The medium containing 2ME2 was removed and replaced with fresh medium after treatment. The number of colonies was determined after further 7 days of incubation. Cells were fixed with absolute methanol for 10 min and stained with 0.5% crystal violet for further 10 min. After washing four times with tap water, the cells were air-dried. The number of colonies was analyzed using Quantity-One (Bio-Rad).

2.4. DNA content analysis

DNA content analysis was performed as previously described [3]. After 2ME2 treatment, cells were washed twice with phosphate buffered saline (PBS) and harvested by trypsinization. Both adherent cells and floating cells were collected and fixed with cold ethanol (70%) for at least 1 h at 4 °C. The fixed cells were washed with PBS before staining with propidium iodide (1 mg/ml) in the presence of RNase A (10 mg/ml). Fluorescence profiles of the stained cells were analyzed by FACSCalibur flow cytometer (Becton Dickinson). Laser with a wavelength of 488 nm was used for excitation and the fluorescence signal was detected with the FL-2 channel. At least 10,000 events were counted.

2.5. Cell growth assay

Exponentially growing HK-1 (2×10^5 cells/dish) cells were plated in 100 mm tissue culture dishes. After overnight incubation, cells were exposed to 10 μM 2ME2 at 37 °C for 24–72 h. Appropriately diluted DMSO was used as solvent control. The total number of viable cells was determined by staining the cells with trypan blue (0.25%). The experiment was performed in triplicates. The results were expressed as mean ± standard deviation. Student's *t*-test in SPSS 11 software program was used for statistical analysis.

2.6. Detection of reactive oxygen species

ROS was detected as previously described [3]. Briefly, 2ME2-treated HK-1 cells were incubated with ROS sensitive probes 2′,7′-dichlorodihydrofluorescein diacetate (H_2DCFDA, 10 μM) for 30 min or dihydroethidium (DHE, 1 μM) for 15 min. The cells were then harvested by trypsinization and washed at least three times with PBS to remove the excessive probes. Oxidized DCF-DA or DHE was analyzed using the FACSCalibur flow cytometer (Becton Dickinson). Laser with a wavelength of 488 nm was used for excitation. Fluorescence signals of the oxidized DCF-DA and oxidized DHE were detected by the FL-1 and FL-2 channels, respectively. At least 10,000 events were counted.

2.7. Immunoblot analysis

After 2ME2 treatment, cells were washed twice with PBS and lysed with lysis buffer containing 250 mM Tris–HCl (pH 8), 1% NP-40 and 150 mM NaCl. Equal amounts of lysates were subjected to electrophoresis on 10% SDS–polyacrylamide gel using Mini-PROTEAN® 3 electrophoresis system (Bio-Rad). After electrophoresis, the separated proteins were transferred to a PVDF transfer membrane (PolyScreen®) and probed with the corresponding primary and secondary antibodies. The membrane was then developed with the WESTSAVE UP™ (Labfrontier Co. Ltd. Bio Division) and the signals were visualized on the X-ray film (Galen).

2.8. Immunofluorescence staining

HK-1 cells were plated onto cover slips in wells of 24-well plates and treated with 10 μM 2ME2 for 48 h. After treatment, cells were washed twice with PBS and fixed with 4% paraformaldehyde in PBS at room temperature for 15 min. The fixed cells were then treated with 0.2% Triton X-100 in PBS for 10 min. After membrane permeabilization, the cells were incubated overnight with anti-β tubulin antibodies (1:200) at 4 °C. After washing five times with PBS, the cells were incubated with fluorescent phycoerythrin-conjugated secondary antibodies (1:200) for 3 h. The cells were washed to remove the unbound secondary antibodies and the nucleus was then counterstained with DAPI (0.5 μg/ml) for 10 min in the dark. Immunofluorescence signals were visualized under a laser scanning confocal microscope (Olympus Fluoview 1000).

2.9. Preparation of metaphase spreads

Metaphase spreads were prepared as previously described [23]. Briefly, HK-1 cells were treated with or without 2ME2 (10 μM) for

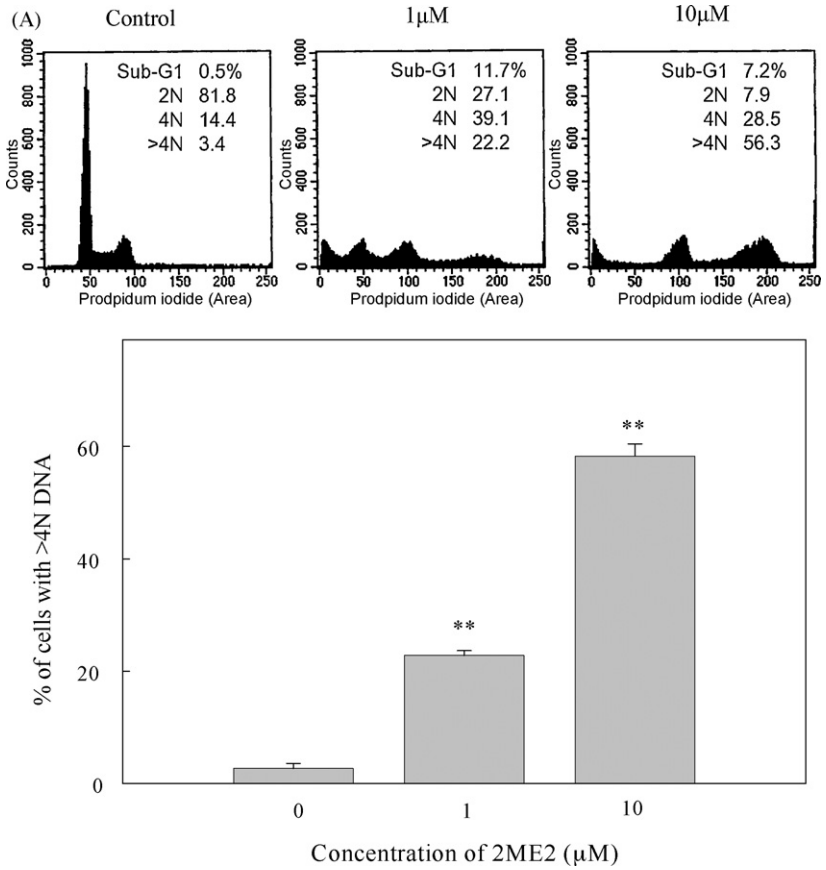

Fig. 2. Kinetics and dose–response of 2ME2-treated HK-1 cells. (A) HK-1 cells (3×10^5/well in 6-well plate) were exposed to 2ME2 (1 or 10 μM) for 48 h and the DNA content was analyzed by flow cytometry. Upper panel: a representative diagram showing the profile of DNA analysis. Lower panel: percentage of cells showing >4N DNA content. Results were expressed as mean ± SD from 3 independent experiments. $^{**}p < 0.01$. (B) HK-1 cells were treated with 10 μM of 2ME2 and the DNA content analysis was performed at various times after 2ME2 treatment. (C) Induction of endoreduplication in HK-1, EBV HK-1 and C666-1 cells. Cells were treated with 10 μM of 2ME2 and the DNA content analysis was performed at 48 h after treatment.

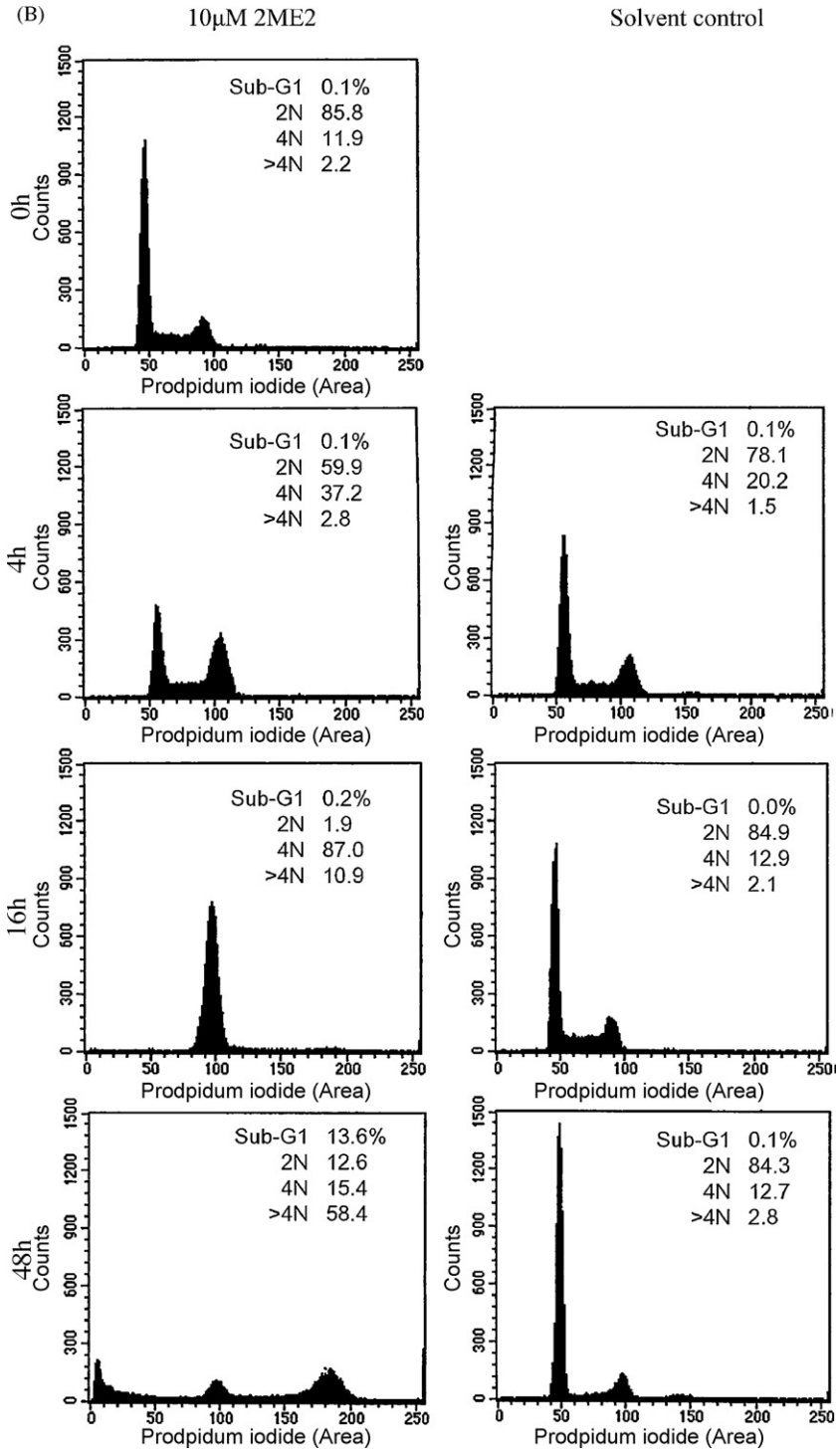

Fig. 2. (*Continued*).

24–48 h. The cells were then incubated with colcemid (0.1 μg/ml, Sigma) for 45 min. After incubation, KCl (0.075 M) was added to the culture and the cells were further incubated for 20 min at 37 °C. The cells were fixed with methanol/acetate acid (3:1, v/v) for at least 30 min. The fixed cells were then dropped onto a glass slide and air-dried. Chromosomes on the slides were stained with DAPI and the fluorescent signals were captured using SPOT software (Sterling Heights, MI, USA) on an OLYMPUS BX51 microscope (Tokyo, Japan).

2.10. Measurement of SOD activity

After 2ME2 treatment, the cells were trypsinized and washed twice with cold PBS. The cells were then resuspended in 10 mM phosphate buffer (pH 7) with 1% Triton X-100. The activity of cellular SOD was measured according to the manufacturer's protocol of the Ransod assay kit from Randox Laboratories Ltd. (Antrim, United Kingdom). The experiments were repeated three times and the results were expressed as mean ± standard

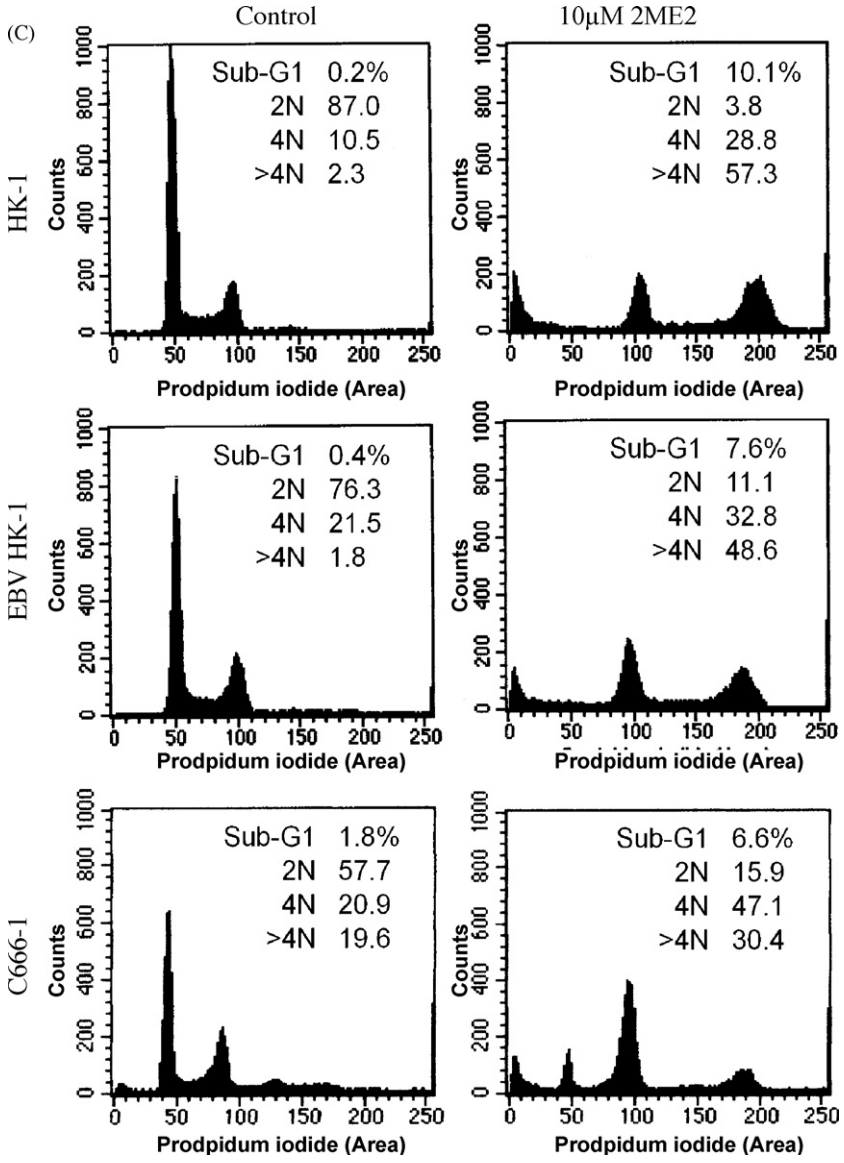

Fig. 2. (*Continued*).

deviation. Student's *t*-test in SPSS 11 software was used for statistical analysis.

2.11. Detection of mitochondrial superoxide

2ME2-treated cells were incubated with 2 μM Mito-HE (MitoSOX™ Red) for 10 min at 37 °C and rinsed three times with PBS. The cells were observed using a laser scanning confocal microscope (Olympus Fluoview 1000) equipped with a multi-line argon laser. Oxidized hydroxyethidium derivative (Mito-OH-Etd) were excited using the excitation wavelength of 543 nm. The 555–592 nm emission filter was used at the emission end for the detection of the fluorescence signals.

2.12. Transfection with MnSOD vector

pcDNA3.1 with a MnSOD cDNA insert, a generous gift from Prof. Abbadie (Institut de Biologie de Lille), was used in this study. HK-1 cells were seeded overnight at a density of 3×10^5 cells/well in 6-well plates. The MnSOD or empty pcDNA3.1 vector (1.6 μg) was transfected into HK-1 cells using Lipofectamine Reagent 2000 (Invitrogen) according to the manufacturer's recommendations. After 24 h of the transfection, the cells were treated with 2ME2 (10 μM) for further 48 h before flow cytometric analysis.

3. Results

3.1. 2ME2 induces endoreduplication in HK-1 cells

HK-1 cells were treated with 2ME2 (10 μM) and the number of viable cells was determined at various times after treatment. The results in Fig. 1A showed that the growth of HK-1 cells was significantly reduced ($p < 0.05$) 1 day after 2ME2 treatment. The cologenicity of 2ME2-treated HK-1 cell was then evaluated (Fig. 1B). Significant re-growth of 2ME2-treated HK-1 cell was not observed. Further microscopic and flow cytometric examinations revealed that the size of the cell body (FSC) and also the granularity of the cell (SSC) were increased at 24–48 h after 2ME2 treatment (Fig. 1C). Cytogenetic analysis was also performed to determine the chromosome number in 2ME2-treated HK-1 cells. The results in Fig. 1D show that the number of metaphase chromosome in the untreated HK-1 cells was increased from 64 to

128 in 2ME2-treated HK-1 cells, suggesting that 2ME2 induced endoreduplication of the HK-1 cells.

The dose–response and the kinetics of endoreduplication were further determined by flow cytometric method. The results in Fig. 2A show that 2ME2 dose dependently increase the >4N population. DNA content also time dependently increased in 2ME2-treated HK-1 cells (Fig. 2B). The percentage of HK-1 cells with 2N DNA content was reduced from 86% in the control HK-1 cells to 60% at 4 h after 2ME2 treatment. The percentage of cells with 4N DNA content was accordingly increased to 37% after 2ME2 treatment, indicating that 2ME2 induced G2/M cell cycle arrest in HK-1 cells. The percentage of cells with >4N DNA content was similar to the control group. Prolonged treatment of HK-1 cells with 2ME2 resulted in a further increased in the DNA content. By 48 h, the percentage of 2ME2-treated HK-1 cells with >4N DNA content was increased to 58%. Prolonged treatment of HK-1 cells with 2ME2 also resulted in the appearance of apoptotic cells (sub-G1). Further increase in the DNA content was not observed after 72 h of 2ME2 treatment (data not shown). The results in these studies indicate that 2ME2 not only induces G2/M cell cycle arrest but also endoreduplication in the HK-1 cells. The endoreduplication-inducing activity of 2ME2 on the EBV harboring HK-1 cells (EBV HK-1) and undifferentiated C666-1 NPC cells was also analyzed. Cells with >4N DNA content were significantly increased in EBV HK-1 and C666-1 at 48 h after 2ME2 (10 μM) treatment (Fig. 2C). As 2ME2 also induced endoreduplication in other NPC cell lines, HK-1 cell line was used in subsequent mechanistic studies.

3.2. 2ME2 induces oxidative stress in HK-1 cells

Many anticancer agents cause cellular injury and stress response through the induction of oxidative stress [24]. To assess

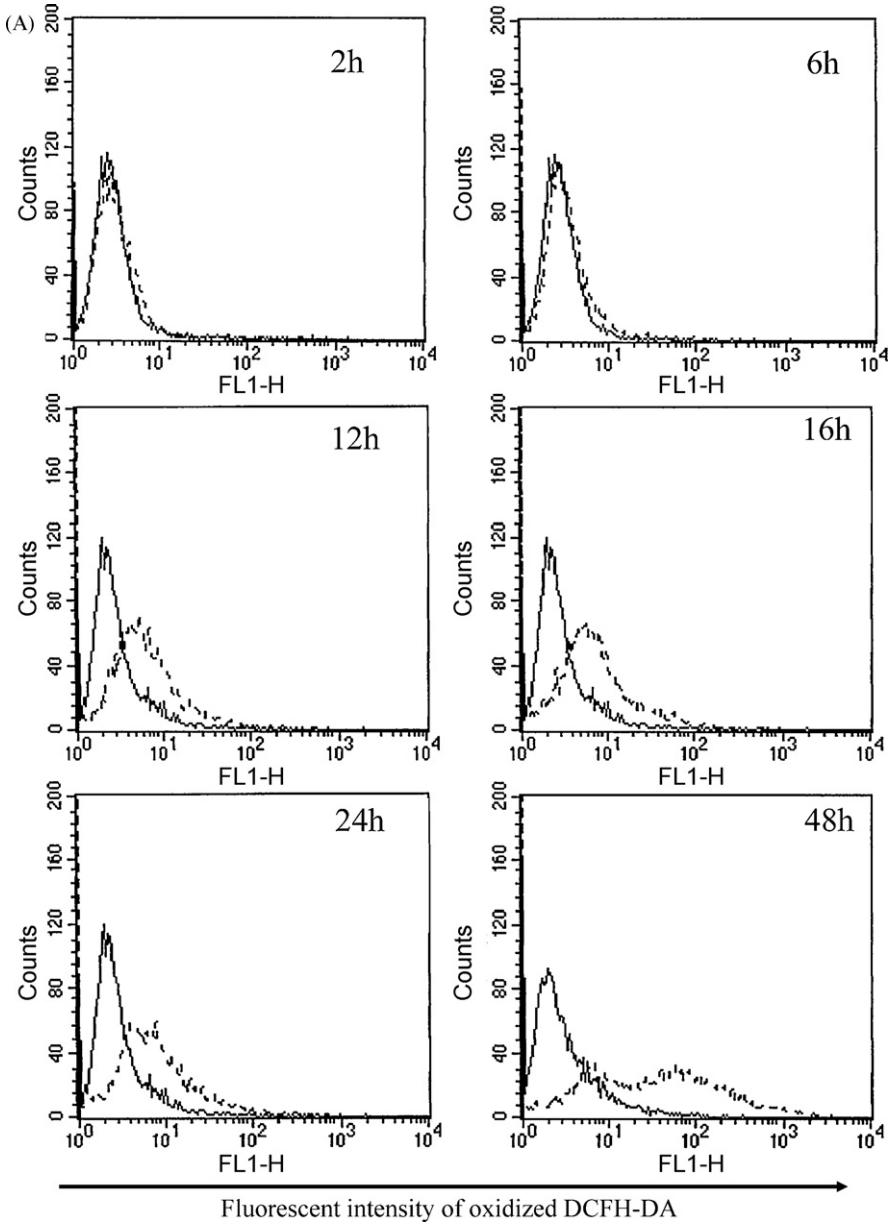

Fig. 3. Detection of ROS in 2ME2-treated HK-1 cells. HK-1 cells (3×10^5 cells/well in 6-well plate) were exposed to the 10 μM 2ME2 for 2–48 h. (A) Cells were then incubated with 10 μM DCFH-DA at 30 min before harvesting. The oxidized DCFH-DA was detected with FL-1 channel. (B) At 15 min before cell harvesting, 1 μM DHE was added into the culture. Fluorescence signals from the fluorescence probe DHE were detected with FL-2 channel. Solid line: untreated HK-1 cells; dotted line: 2ME2-treated HK-1 cells. (C) Confocal images of mitochondrial superoxide sensor MitoSOX in 2ME2-treated HK-1 cells. 2ME2 (10 μM) treated HK-1 cells were labeled with MitoSOX for 10 min before cell harvesting for image analysis.

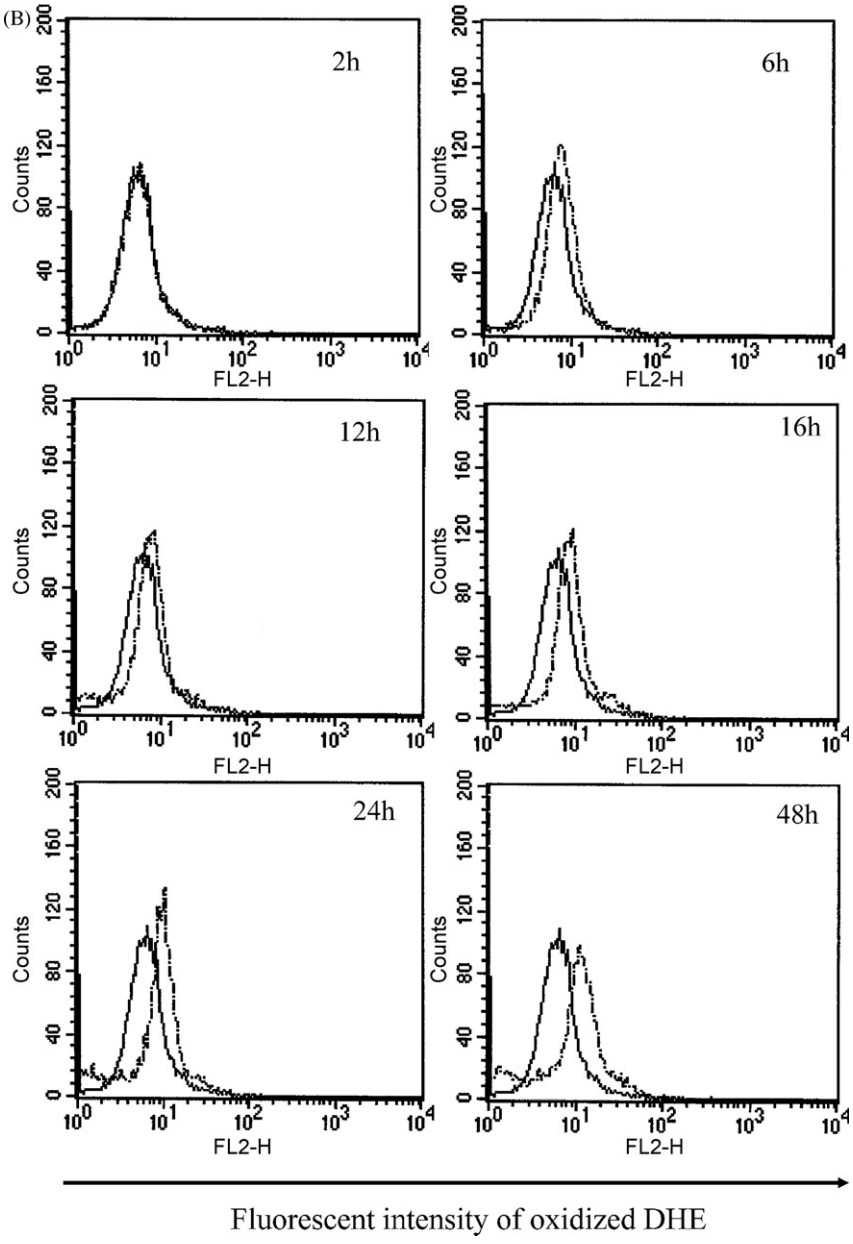

Fig. 3. (*Continued*).

whether oxidative stress was induced in 2ME2-treated HK-1 cells, the production of intracellular ROS was monitored by labeling 2ME2-treated HK-1 cells with H_2DCFDA, a fluorescent probe sensitive to ROS such as H_2O_2, $^{\bullet}OH$, and $ONOO^-$. In addition, the production of intracellular superoxide anions was measured by labeling cells with a specific superoxide anion probe, DHE. A time-dependent increase in fluorescence signals of both oxidized DCF and DHE fluorescence probes was observed in cells after treatment with 2ME2 (Fig. 3A and B), indicating that 2ME2 induced oxidative stress in HK-1 cells. Mitochondria play an integral role in cellular metabolism and are the source of superoxide. 2ME2-induced generation of superoxide in mitochondria was further determined using a mitochondria-targeted superoxide sensitive probe Mito-SOX. A time-dependent increase in the fluorescence signal of MitoSOX was observed in 2ME2-treated HK-1 cells (Fig. 3C). To further verify the role of superoxide in endoreduplication, HK-1 cells were treated with superoxide anion donor, DMNQ (10 μM), and the production of endoreduplicating cells was measured at 48 h after treatment. The results in Fig. 4 show a significant increase in the number of endoreduplicating cells after treatment of DMNQ. Taken together, 2ME2 was found to increase oxidative stress, including the oxidative stress in mitochondria, in HK-1 cells.

3.3. 2ME2-induced oxidative stress is correlated with the decline in SOD activity

To further evaluate the role of oxidative stress in 2ME2-induced endoredulpication of HK-1 cells, the activity of SOD in 2ME2-treated HK-1 cells was examined. The results in Fig. 5 show that the activity of SOD was significantly inhibited at 14–48 h after 2ME2 treatment ($p < 0.05$). The inhibition of SOD activity was correlated with the appearance of oxidative stress in HK-1 (Fig. 3).

3.4. Prevention of 2ME2-induced endoreduplication by SOD mimetic TEMPO or MnSOD overexpression

Next, we determined whether endoreduplication could be reduced by reducing oxidative stress in 2ME2-treated HK-1 cells.

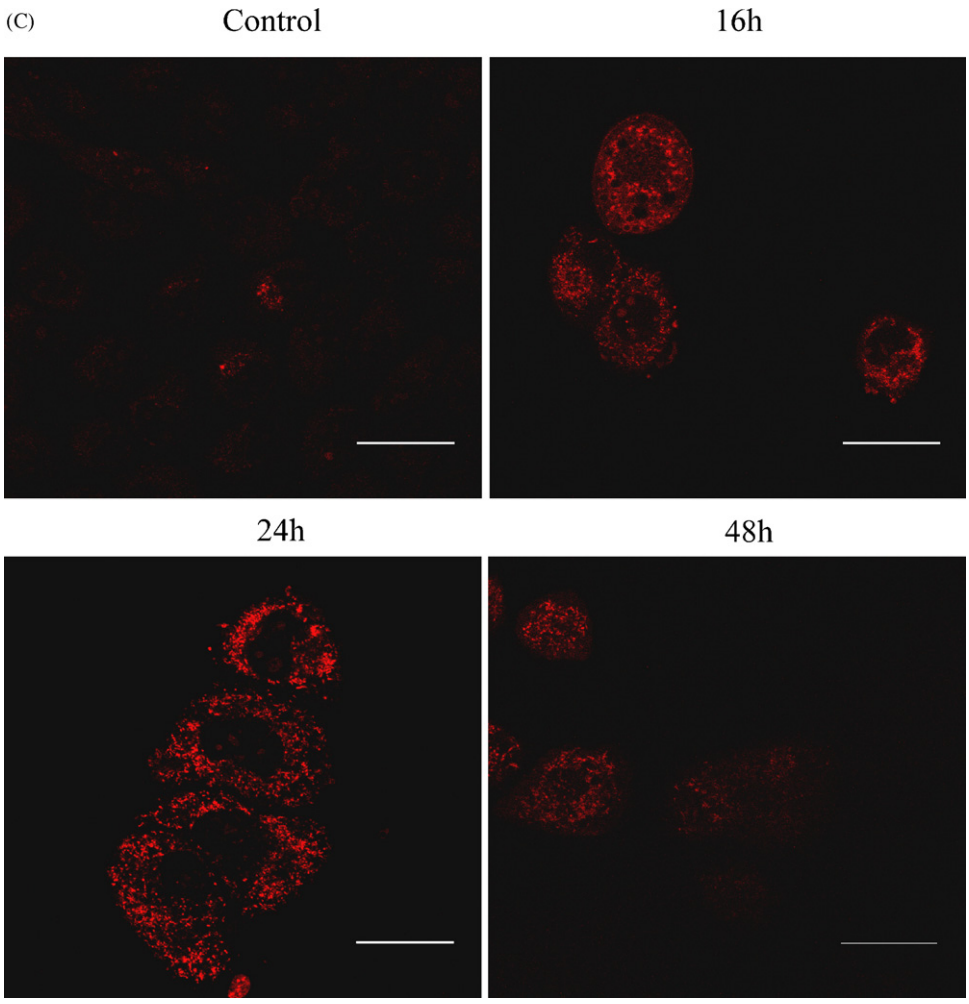

Fig. 3. (*Continued*).

First of all, HK-1 cells were pre-treated with SOD mimetic TEMPO for 1 h before the 2ME2 treatment. Oxidative stress was then evaluated by using the ROS sensitive intracellular probes H_2DCFDA and DHE. The results in Fig. 6A show that oxidative stress in 2ME2-treated HK-1 cells was reduced, as judged from the shift of the fluorescence peak to the left, by TEMPO. The reduction of oxidative stress was accompanied by a reduction of endoreduplicating cells (Fig. 6B). The percentage of >4N population was reduced from 51.9% (2ME2 alone) to 4.6% (2ME2 + TEMPO). As MnSOD is know to play a cyto-protective role in mitochondria, we

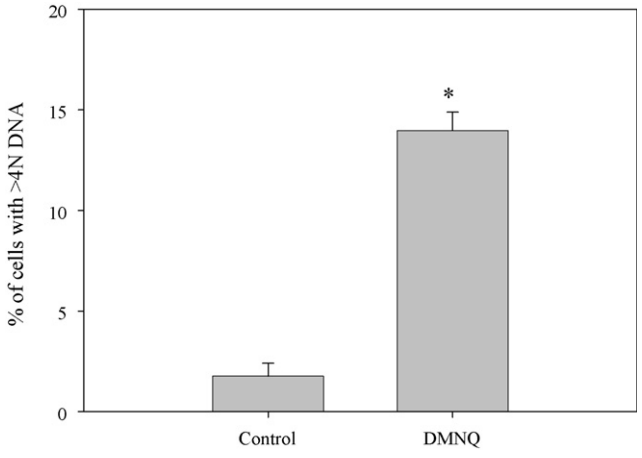

Fig. 4. Induction of endoreduplication by superoxide anion donor DMNQ. HK-1 cells (3×10^5 cells/well in 6-well plate) were exposed to 10 μM DMNQ for 48 h and the DNA content was analyzed by flow cytometry. Results were expressed as mean ± SD from 3 independent experiments. $^*p < 0.05$.

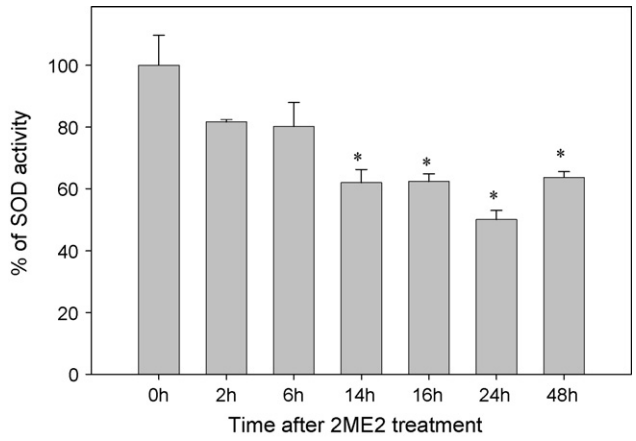

Fig. 5. Reduction of SOD activity in 2ME2-treated HK-1 cells. HK-1 cells (1×10^6/dish) were exposed to the 10 μM 2ME2 for 2–48 h. SOD activity was determined as described in Section 2. $^*p < 0.05$.

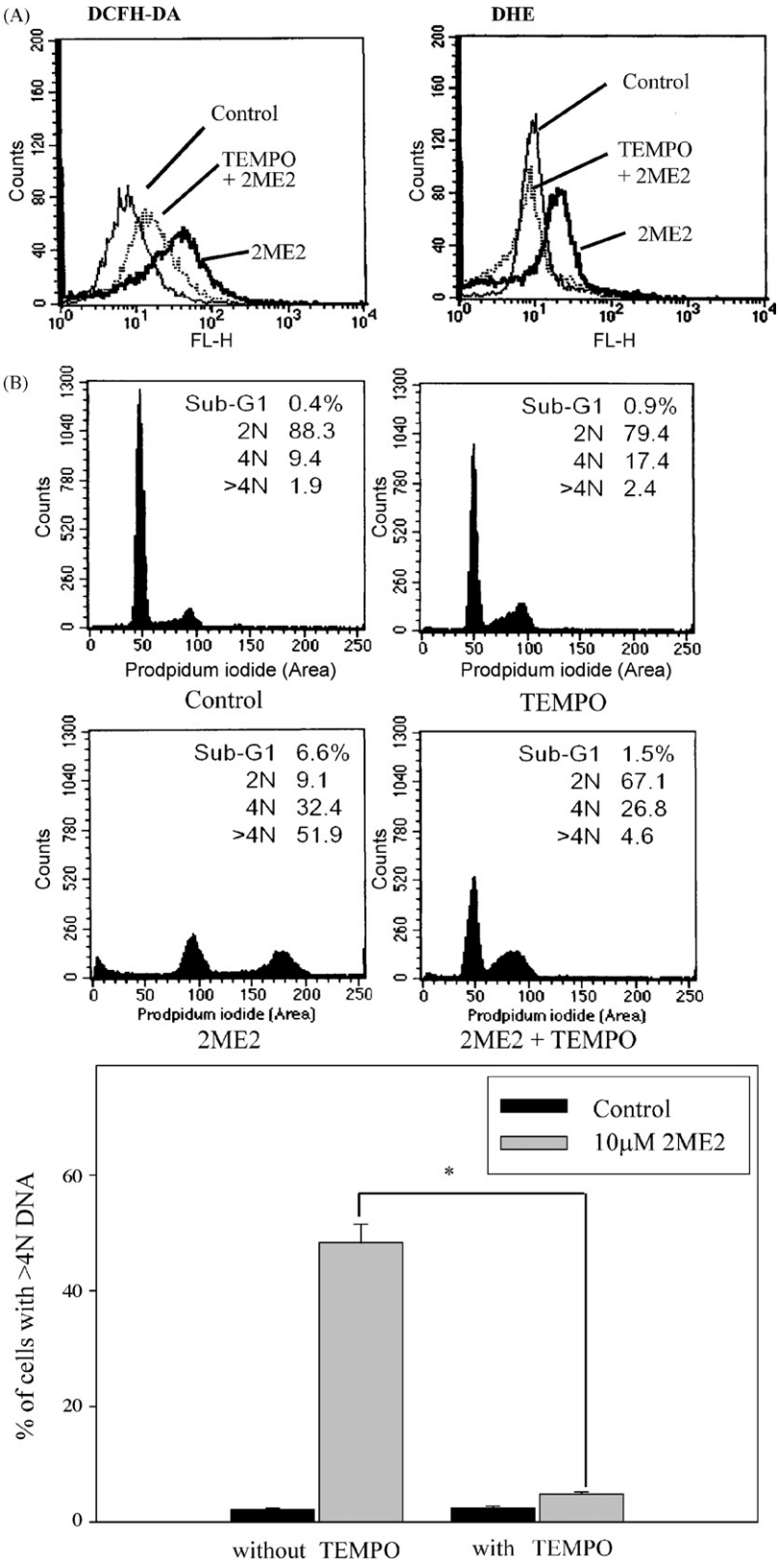

Fig. 6. Role of MnSOD in 2ME2-induced endoreduplication. (A) Reduction of 2ME2-induced oxidative stress by SOD mimetic, TEMPO. HK-1 cells (3×10^5/well in 6-well plate) were pre-incubated with TEMPO (2 mM) for 1 h before treating with 10 μM 2ME2 for 16 h. DCFH-DA or DHE was added at 30 or 15 min, respectively, before cell harvesting. Fluorescence signals from oxidized DCFH-DA and DHE were analyzed with FL-1 and FL-2 channels, respectively. (B) Reduction of 2ME2-induced endoreduplication by TEMPO. HK-1 cells were pre-treated with 2 mM TEMPO for 1 h before exposure to 2ME2 for 48 h. Both floating and adherent cells were collected for DNA content analysis. Upper panel: representative flow profile. Lower panel: statistical analysis on the reduction of endoreduplication by TEMPO. $^*p < 0.05$. (C) Western blotting analysis of MnSOD in HK-1 cells transiently transfected with MnSOD–pcDNA3.1. Control HK-1 received the empty plasmid. (D) Reduction of 2ME2-induced endoreduplication of HK-1-MnSOD cells in MnSOD overexpressed HK-1 cells. Upper panel: representative profiles of 2ME2-induced endoreduplication in MnSOD transfected HK-1 cells. Cells were analyzed at 48 h after 2ME2 treatment. Both floating and adherent cells were collected for flow cytometric analysis. Lower panel: statistical analysis of >4N cells in 2ME2-treated cells overexpressing MnSOD. Results were expressed as mean ± SD of 3 independent experiments. $^*p < 0.05$.

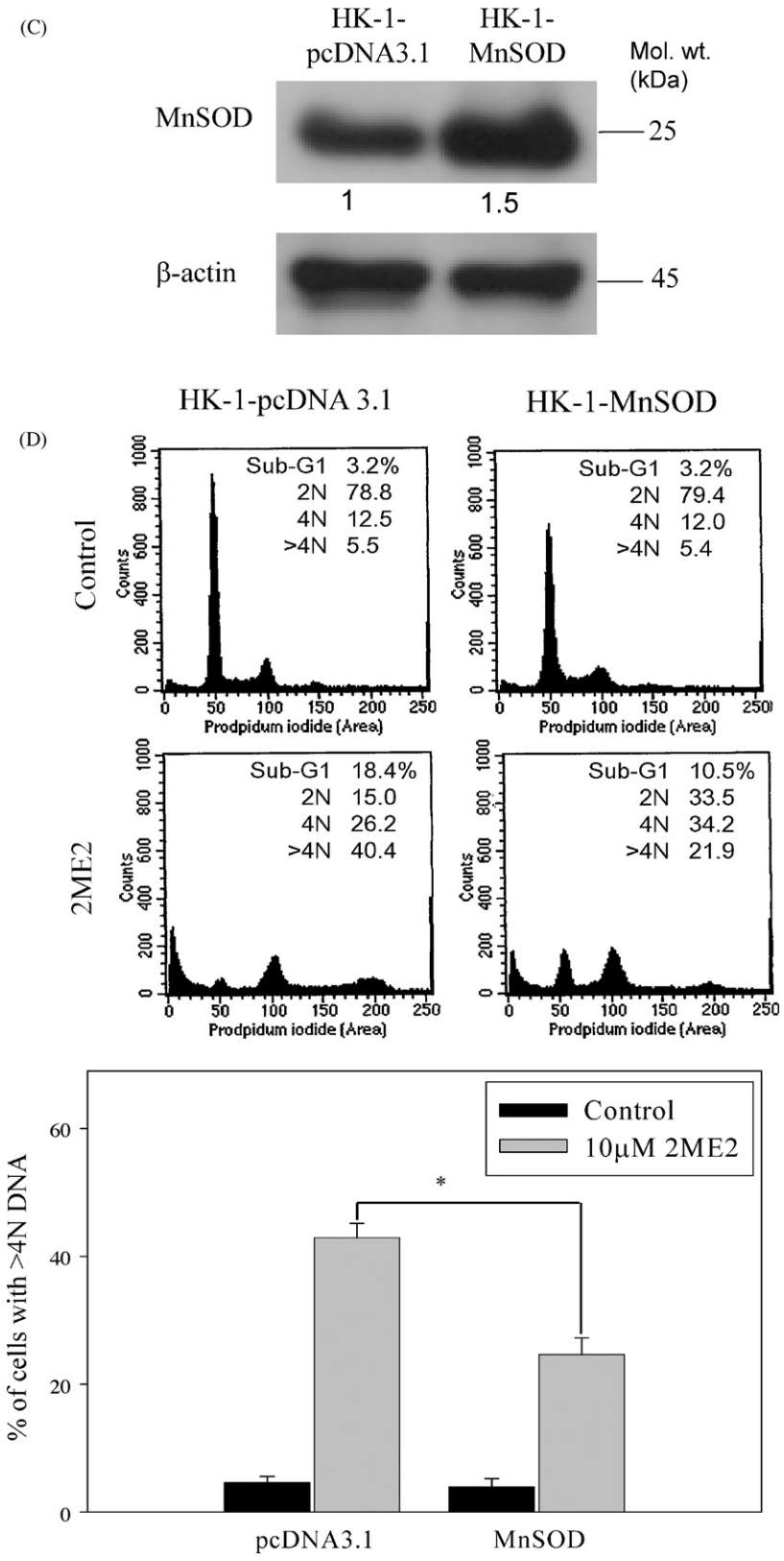

Fig. 6. (*Continued*).

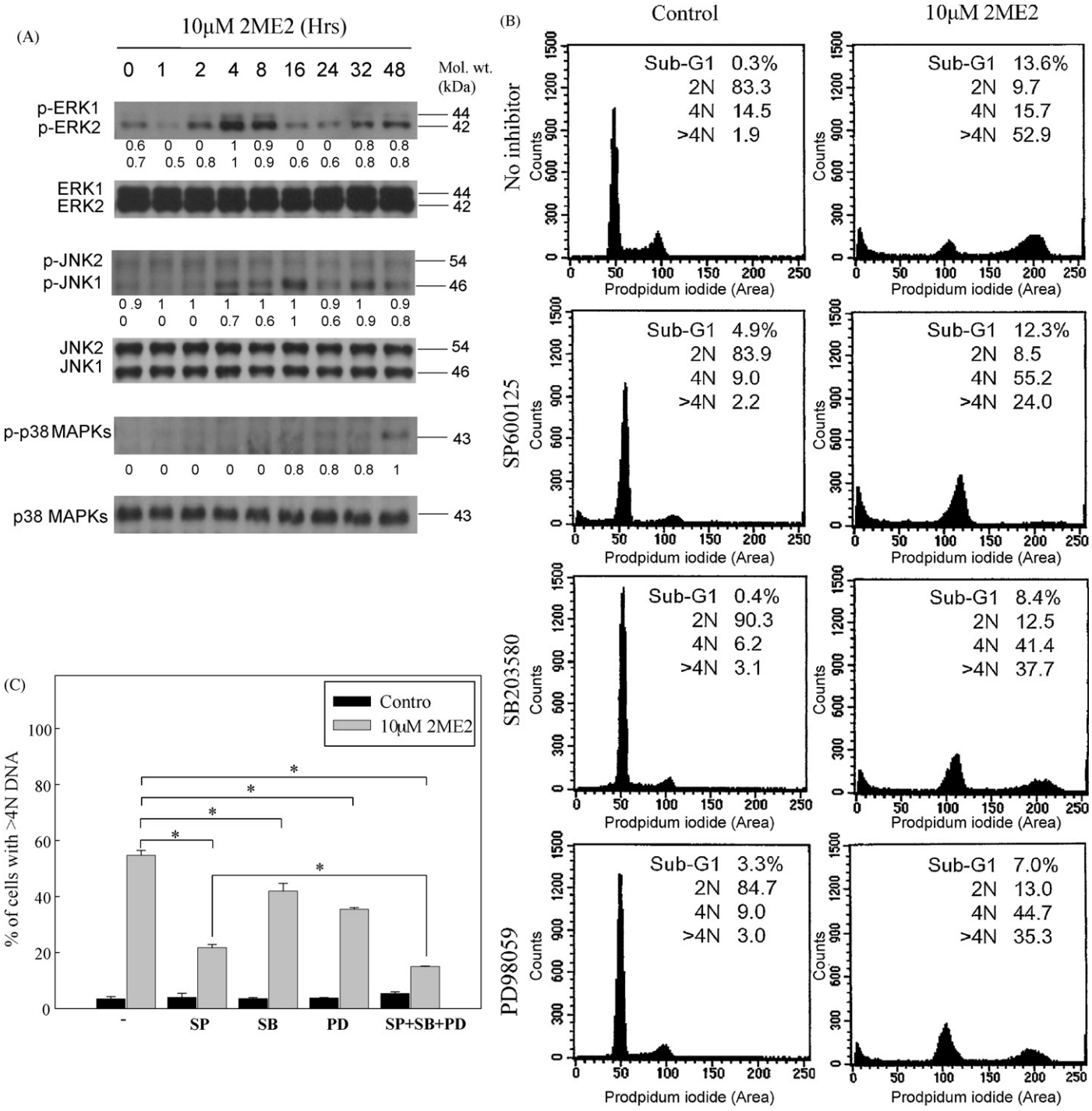

Fig. 7. Activation of MAPK signaling pathways in 2ME2-treated HK-1 cells. HK-1 cells were seeded at a density of 3×10^5 cells per well in 6-well plates for overnight. Cells were then incubated with 10 μM 2ME2 for various times. (A) Western blotting analysis of 2ME2-induced activation of MAPKs. Total cell lysates were prepared at various times (0–48 h) after 2ME2 treatment. The numbers at the bottom of the blot represent the values of densitometric scanning of the p-ERK1, p-ERK2, p-JNK1, p-JNK2 and p-p38 MAPKs. The values were normalized with reference to the total non-phosphorylated form. (B) Effect of JNK inhibitor SP600125 (10 μM), p38 MPAKs inhibitor SB203580 (10 μM) and MEK inhibitor PD98059 (30 μM) on 2ME2-induced endoreduplication of HK-1 cells. HK-1 cells were pre-treated with inhibitors at 1 h before 2ME2 treatment. Cells were analyzed at 48 h after 2ME2 treatment. (C) The percentage of cells with >4N DNA content in bar chart was expressed as mean ± SD of three independent experiments. Student's *t*-tests were performed for determination of the significant difference, $^*p < 0.05$.

then further examined the effect of MnSOD overexpression in 2ME2-induced endoreduplication. Transfection of HK-1 cells with MnSOD–pcDNA3.1 resulted in an approximately 50% increase in the expression of MnSOD (Fig. 6C). The increase in MnSOD overexpression is correlated with the reduced generation of endoreduplicating cells after 2ME2 treatment (Fig. 6D).

3.5. Analysis of MAPK signaling pathways in 2ME2-treated HK-1 cells

Members of the MAPK family have been reported to play a crucial role in the regulation of cell cycle [25]. However, the role of MAPKs in endoreduplication was not fully studied. The involvement of MAPKs in 2ME2-induced endoreduplication of HK-1 cells

was then examined. Fig. 7A shows the kinetics of appearance of phosphorylated ERK (p-ERK1/2), phosphorylated JNK (p-JNK1/2) and phosphorylated p38 MAPKs (p-p38 MAPKs) in 2ME2-treated HK-1 cells. Two waves of increase in p-ERK1/2 were observed at 2–8 h and 32–48 h after 2ME2 treatment. Similarly, two waves of increase in p-JNK1 (16 and 32 h) were observed after 2ME2 treatment. However, the level of p-JNK2 in 2ME2-treated HK-1 cells was similar to that of the untreated HK-1 cells. For the p38 MAPKs, the expression levels of p-p38 MAPKs were initially detected at 16–32 h, and the level was further increased at 48 h after 2ME2 treatment.

To determine the possible role of MAPK activation in the induction of endoreduplication, HK-1 cells were pre-treated with inhibitors for MEK/ERK, JNK and p38 MAPKs before 2ME2 treatment. The results in Fig. 7B show that the percentage of endoreduplicating cells was reduced from 52.9% in the 2ME2 treatment group to 35.3%, 24% and 38% by 30 μM PD98059 (MEK/ERK inhibitor), 10 μM SP600125 (JNK inhibitor) and 10 μM SB203580 (p38 MAPK inhibitor), respectively. The degree of reduction of endoreduplication by SP600125 was greater than those of PD98059 and SB203580. The combined treatment of cells with SP600125, SB203580 and PD98059 further reduced the number of endoreduplicating cells. This observation suggested that inhibition of MAPKs could attenuate 2ME2-induced endoreduplication (Fig. 7C).

3.6. Role of oxidative stress in 2ME2-induced activation of MAPKs

To further establish the relation between the induction of oxidative stress, activation of MAPKs and the induction of endoreduplication, Western blotting analysis was performed to examine the expression of p-ERK1/2, p-JNK1/2 and p-p38 MAPKs in cells with TEMPO pre-treatment. As oxidative stress was initially detected at 12 h (Fig. 3) and p-ERK, p-JNK and p-p38 MAPKs were differentially expressed (Fig. 7) after the appearance of oxidative stress, 2ME2-treated HK-1 cells were then harvested and analyzed at 16 h (for p-JNK) and 48 h (for p-ERK and p-p38 MAPKs). The results in Fig. 8 show that the expression level of p-JNK1 was greatly reduced in 2ME2-treated cells with TEMPO pre-treatment. However, p-ERK1/2 and p-p38 MAPKs did not have any obvious changes after pre-treatment of TEMPO, suggesting that oxidative stress is involved in the expression of p-JNK.

3.7. Microtubule organization in 2ME2-treated HK-1 cells

Although 2ME2 has previously been shown to disrupt the microtubule dynamics by binding to the colchicine site of tubulin [11], the role of oxidative stress in 2ME2-induced microtubule disruption has not been fully studied. To evaluate the effect of 2ME2-induced oxidative stress on the microtubule organization in HK-1 cells, the cells were stained with anti-beta-tubulin antibody. A clear pattern of microtubule organization was seen in the control HK-1 cells (Fig. 9). The treatment of the cells with 2ME2 resulted in the disappearance of the tubulin filaments in the cytoplasm. In the presence of TEMPO, a clear staining of tubulin filaments was observed in 2ME2-treated HK-1 cells, and the results were correlated with the reduction of endoreduplication in the HK-1 cells (Fig. 6B). To further establish the link between the production of superoxide anion, activation of JNK signaling and the organization of tubulin filaments, we then examined the staining of tubulin filaments in DMNQ-treated HK-1 cells. Similar to the 2ME2-treated HK-1 cells, a clear pattern of tubulin organization was not seen in DMNQ-treated NPC cells. The organization of the filament was restored in cells pre-treated with the JNK inhibitor SP600125. The results from this study indicate that JNK is involved in DMNQ-induced disruption of the tubulin filaments (Fig. 10).

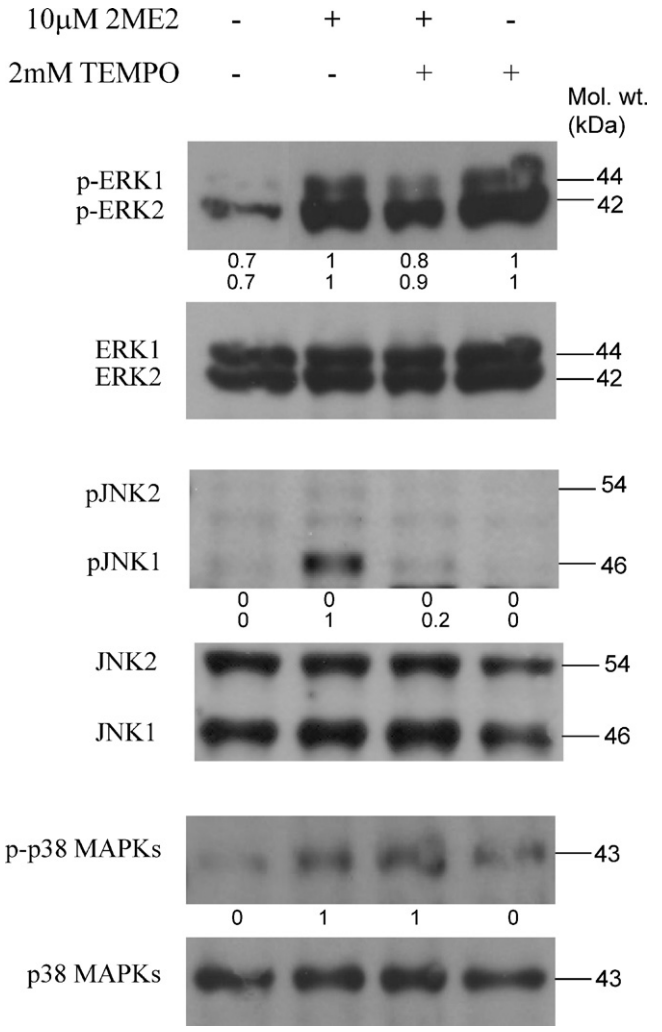

Fig. 8. Effect of TEMPO on the expression of phosphorylated JNK, ERK and p38 MAPKs. HK-1 cells (3×10^5/well in 6-well plate) were pre-incubated with TEMPO (2 mM) for 1 h before treating with 10 μM 2ME2. Total cell lysates were then prepared at 16 (for JNK) and 48 h (for ERK and p38 MAPKs) after 2ME2 treatment. Western blotting analysis was performed as described in Section 2. The numbers at the bottom of the blot represent the values of densitometric scanning of the p-ERK1, p-ERK2, p-JNK1, p-JNK2 and p-p38 MAPKs. The values were normalized with reference to the total non-phosphorylated form.

4. Discussion

2ME2, an estradiol metabolite with anti-proliferative and anti-angiogenic activity, is regarded as a novel anticancer agent. Most of the previous studies demonstrated that the cell growth inhibitory effect of 2ME2 is due to the induction of cell cycle arrest and apoptosis in the tumour cells [26,27]. With regard to NPC cells, previous studies also reported that 2ME2 effectively induced apoptosis and cell cycle arrest at G2/M phase [3,28]. In the present study, we demonstrate that 2ME2 induces not only G2/M cell cycle arrest, but also the endoreduplication in the well-differentiated HK-1 NPC cells. The close association between EBV infection and NPC is well documented [29]. In the present study, we have also examined the endoreduplication-inducing effect of 2ME2 on EBV HK-1 and another NPC C666-1 cell line. Our results clearly showed that similar endoreduplication-inducing effect was also observed in these two cell lines.

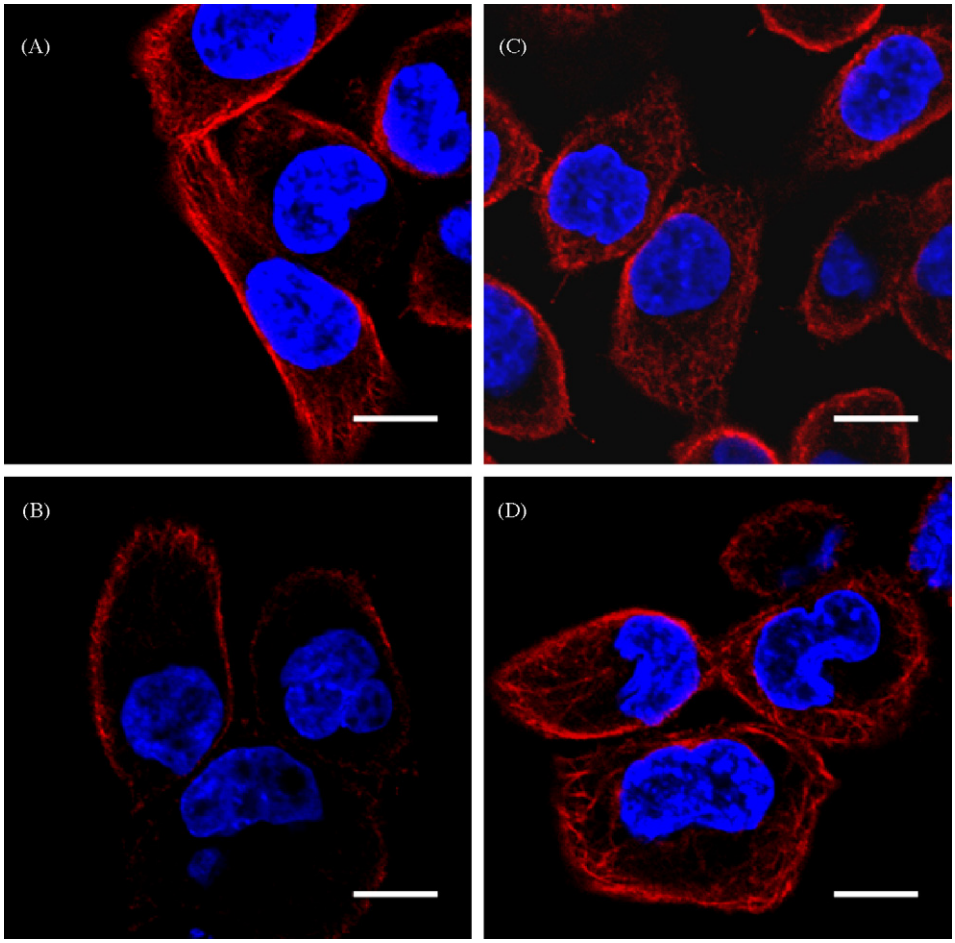

Fig. 9. Immunostaining of β-tubulin in 2ME2-treated HK-1 cells. HK-1 cells (2×10^4 cells/cover slip) were incubated in wells of 24-well plate for overnight. The cells were then treated with 2ME2 (10 μM) for 48 h before immunostaining with anti-tubulin antibody as described in Section 2. (A) Control, (B) 2ME2, (C) TEMPO (2 mM) and (D) 2ME2 + TEMPO (2 mM) pre-treatment. Nucleus was counterstained with DAPI. Scale bar = 10 μm.

Endoreduplication, a variant of the cell cycle, is the process by which the content of DNA is increased without accompanying division [30]. Drug-induced endoreduplication in tumour cells has not been fully studied. An earlier study with microtubule inhibitor showed that nocodazole induced endoreduplication of the human colon HCT16 carcinoma cell [14]. The cell cycle regulator Cdk inhibitor $p21^{Waf/Cip\ 1}$ was found to play a role in the regulation of endoreduplication. The involvement of $p21^{Waf/Cip\ 1}$ was also observed in Paclitaxel-treated prostate cancer cells [13]. In human breast epithelial HBL-100 cells, indirubin-3′-monoxime was found to induce endoreduplication through the inhibition of Cdk/cyclin B [31]. The endoreduplication-inducing effect has recently been reported in human smooth muscle cells [32,33]. The endoreduplication-inducing effect in primary smooth muscle cells was associated with the increase in kinase activity of Cdk2 [33]. Apart from the targeting of microtubule and cell cycle regulators, DNA damaging agent cisplatin has recently been shown to induce endoreduplication in DHD-K-12 colon carcinoma cells [34]. However, the signaling mechanism of induction in these studies was not examined in detail.

MAPK signaling pathways are known to play a crucial role in proliferation, differentiation, development, transformation and apoptosis [35]. ERK is generally considered to regulate cell growth and cell proliferation, while JNK and p38 MAP kinases are involved in programmed cell death [36]. However, the role of MAPK signaling pathways in endoreduplication has not been fully established. In the present study, we found that the phosphorylated forms of ERK, JNK and p38 MAPKs were all differentially upregulated in cells at various times after 2ME2 treatment. The involvement of these three signaling pathways was evidence as the percentage of endoreduplicating cells was reduced when the cells were pre-treated with ERK, JNK and p38 MAPK inhibitors. Compared with ERK and p38 MAPKs, maximum reduction of endoreduplication was observed when the cells were pre-treated with JNK inhibitor SP600125. A recent study suggested that the JNK signaling pathway may be involved in the actin depolymerization agent pectenotoxin-2 (PTX-2)-induced endoreduplication of human leukemia cells [37]. Using mantle cell lymphoma cell lines, Wang et al. found that JNK was constitutively activated and inhibition of JNK by SP600125 would cause G2/M arrest and endoreduplication [38]. In the present study, we found that 2ME2 induced endoreduplication through JNK activation. The activation of JNK was correlated with the generation of oxidative stress in the 2ME2-treated HK-1 cells. We have clearly detected the elevation of ROS using the ROS sensitive probes DCFH-DA, DHE and the mitochondrial superoxide sensitive probe MitoSOX in cells after 2ME2 treatment. The specific role of oxidative stress in 2ME2-induced endoreduplication was further confirmed. Firstly, the activity of SOD was reduced in cells after 2ME2 treatment. The endoreduplication-inducing effect was attenuated in cells with overexpression of the mitochondrial enzyme MnSOD or in cells

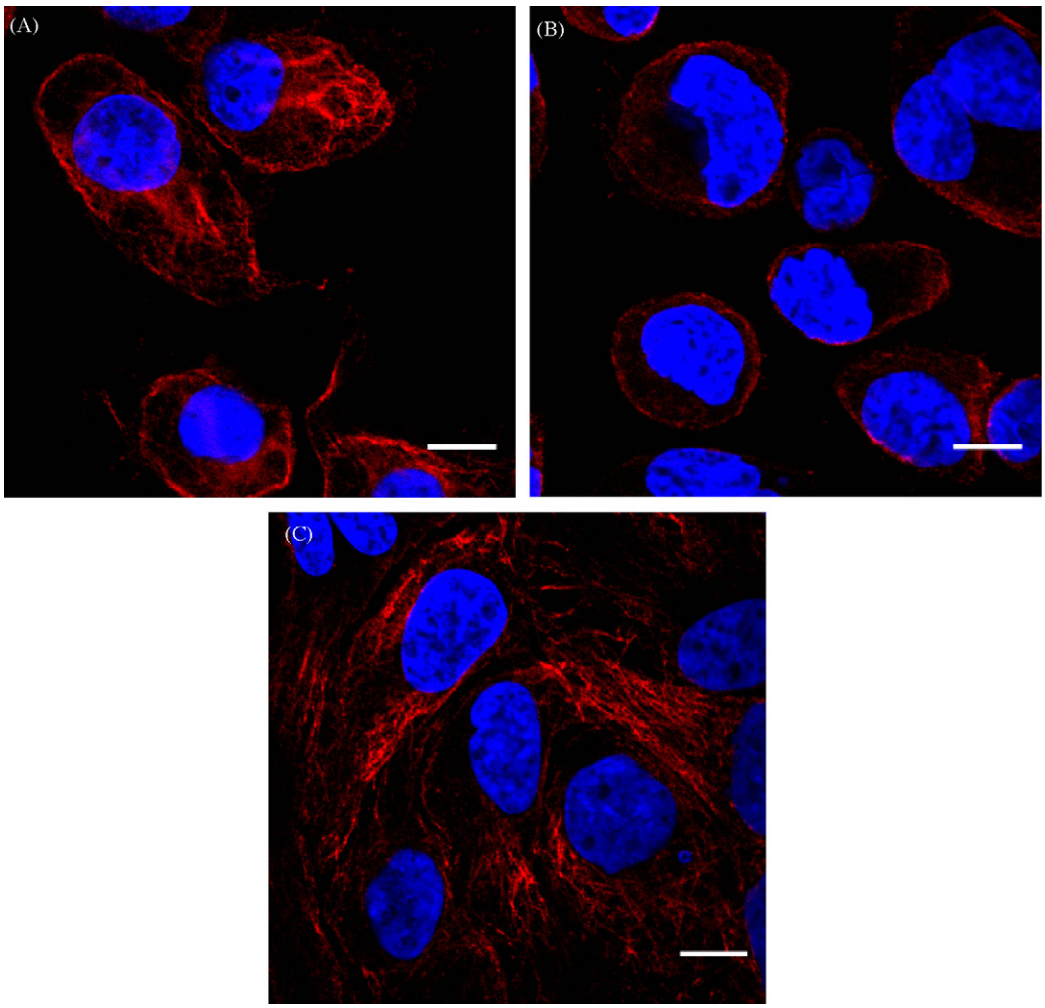

Fig. 10. Immunostaining of β-tubulin in DMNQ-treated HK-1 cells. The cells (2×10^4 cells/cover slip) were treated with DMNQ (10 μM) for 48 h before immunostaining with anti-tubulin antibody as described in Section 2. (A) Control, (B) DMNQ, and (C) DMNQ + SP600125 (10 μM) pre-treatment. Nucleus was counterstained with DAPI. Scale bar = 10 μm.

with SOD mimetic TEMPO pre-treatment. Secondly, the levels of ROS were also reduced in cells with SOD mimetic pre-treatment. The effect was also correlated with the reduction of endoreduplication. Thirdly, 2ME2-induced expression of p-JNK and disruption of microtubule were prevented by TEMPO. This observation is further supported by the recent study that oxidative stress may cause tubulin depolymerization [39]. Although 2ME2-induced endoreduplication could also be reduced by the ERK and p38 MAPK specific inhibitor, the expression of p-ERK and p-p38 MAPKs was not affected by the SOD mimetic. This observation indicates that the activation of ERK and p38 MAPKs is independent of the mitochondrial oxidative stress.

In the present study, the more specific role of superoxide anion in endoreduplication was demonstrated by treating the cells with superoxide anion donor, DMNQ. However, the percentage of endoreduplicating cells was lower than that for 2ME2-treated cells. This observation suggested that the induction of endoreduplication required a concerted sequence of events, such as disruption of microtubules, elevation of mitochondrial superoxide anion and the activation of JNK, phosphorylation of ERK and p38 MAPKs, in 2ME2-treated cells (Fig. 11).

The biological significance of drug-induced endoreduplication is worthy of discuss. First of all, endoreduplication is widespread in plants and insects. In mammals, megakaryocytes and trophoblasts have been shown to increase the DNA content through endocycling [30]. This process normally allows cells to increase their mass or metabolic output. In the chemotherapeutic study of tumour cells, Puig et al. recently found that cisplatin-treated DHD-K12 colon carcinoma cells had undergone depolyploidization and re-grown after endoreduplication [34]. Hence, the process of drug-induced endoreduplication and the subsequent depolyploidization may contribute to the re-growth of tumour after chemotherapy. In case of SV-40 transformed human breast epithelial cells and leukemia cells, indirubin-3′-monoxime or PTX-2-induced endoreduplication was followed by the death of the tumour cells [31,37], and hence contributed to the anti-tumour mechanisms of the drug. In the present study, the re-growth of 2ME2-treated HK-1 cells was not observed in the colony assay. This observation suggests that 2ME2 may be used as an anti-tumour agent for NPC cells. In spite of previous studies on the anti-tumour activities of 2ME2, limited work has been done on 2ME2-induced endoreduplication of the tumour cells. As 2ME2 is currently under various clinical trials [40,41], understanding the signaling mechanisms of drug-induced endoreduplication would not only facilitate the future development of 2ME2 or 2ME2 derivatives [42] for the treatment of malignant diseases, but also facilitate the development of strategies for the prevention of the development of drug resistant cells after chemotherapy, especially treatment with anti-mitotic drugs.

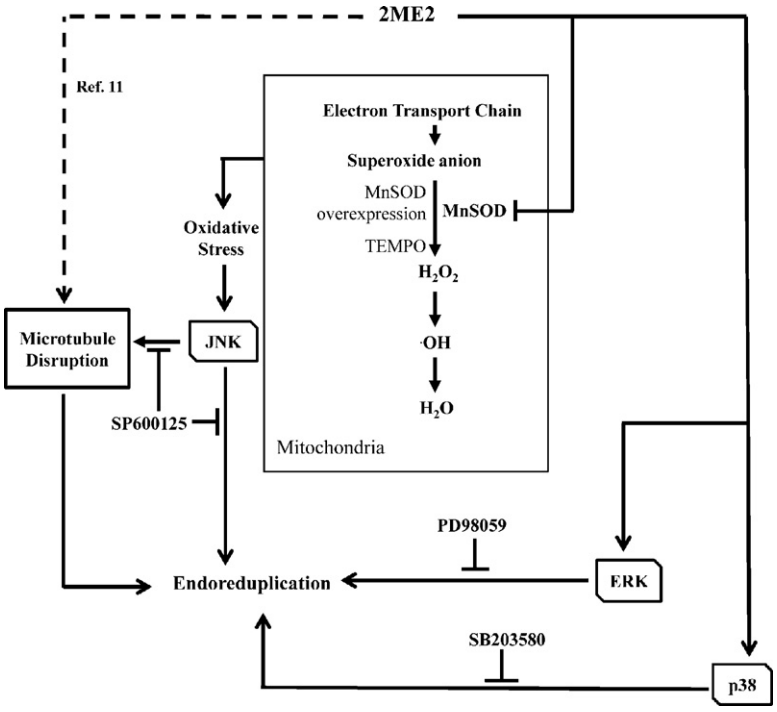

Fig. 11. Proposed mechanism of 2ME2-induced endoreduplication. Dotted line indicates the previously reported anti-microtubule function of 2ME2 (Ref. [11]). Superoxide anions are normally produced at low level during oxygen metabolism. The toxicity of superoxide was neutralized by the mitochondrial MnSOD. Solid line outlines the actions of 2ME2 observed in the present study.

Acknowledgements

This study was partly supported by the following grants: HKBU (FRG2/08-09/076 and FSRS/07-08/02) and RGC (HKBU 1/06C).

References

[1] Sutherland TE, Anderson RL, Hughes RA, Altmann E, Schuliga M, Ziogas J, et al. 2-Methoxyestradiol — a unique blend of activities generating a new class of anti-tumour/anti-inflammatory agents. Drug Discov Today 2007;12:577–84.
[2] Mooberry SL. Mechanism of action of 2-methoxyestradiol: new developments. Drug Resist Updat 2003;6:355–61.
[3] Lee YM, Ting CM, Cheng YK, Fan TP, Wong RN, Lung ML, et al. Mechanisms of 2-methoxyestradiol-induced apoptosis and G2/M cell-cycle arrest of nasopharyngeal carcinoma cells. Cancer Lett 2008;268:295–307.
[4] Park J, Franco RS, Augsburger JJ, Banerjee RK. Comparison of 2-methoxyestradiol and methotrexate effects on non-Hodgkin's B-cell lymphoma. Curr Eye Res 2007;32:659–67.
[5] Thaver V, Lottering ML, van Papendorp D, Joubert A. In vitro effects of 2-methoxyestradiol on cell numbers, morphology, cell cycle progression, and apoptosis induction in oesophageal carcinoma cells. Cell Biochem Funct 2009.
[6] Van Zijl C, Lottering ML, Steffens F, Joubert A. In vitro effects of 2-methoxyestradiol on MCF-12A and MCF-7 cell growth, morphology and mitotic spindle formation. Cell Biochem Funct 2008;26:632–42.
[7] Zou H, Zhao S, Zhang J, Lv G, Zhang X, Yu H, et al. Enhanced radiation-induced cytotoxic effect by 2-ME in glioma cells is mediated by induction of cell cycle arrest and DNA damage via activation of ATM pathways. Brain Res 2007;1185:231–8.
[8] Maran A, Shogren KL, Benedikt M, Sarkar G, Turner RT, Yaszemski MJ. 2-Methoxyestradiol-induced cell death in osteosarcoma cells is preceded by cell cycle arrest. J Cell Biochem 2008;104:1937–45.
[9] Fong YC, Yang WH, Hsu SF, Hsu HC, Tseng KF, Hsu CJ, et al. 2-Methoxyestradiol induces apoptosis and cell cycle arrest in human chondrosarcoma cells. J Orthop Res 2007;25:1106–14.
[10] Bhati R, Gokmen-Polar Y, Sledge Jr GW, Fan C, Nakshatri H, Ketelsen D, et al. 2-Methoxyestradiol inhibits the anaphase-promoting complex and protein translation in human breast cancer cells. Cancer Res 2007;67:702–8.
[11] Liaw TY, Salam NK, McKay MJ, Cunningham AM, Hibbs DE, Kavallaris M. Class I beta-tubulin mutations in 2-methoxyestradiol-resistant acute lymphoblastic leukemia cells: implications for drug–target interactions. Mol Cancer Ther 2008;7:3150–9.
[12] Ganem NJ, Storchova Z, Pellman D. Tetraploidy, aneuploidy and cancer. Curr Opin Genet Dev 2007;17:157–62.
[13] Lanzi C, Cassinelli G, Cuccuru G, Supino R, Zuco V, Ferlini C, et al. Cell cycle checkpoint efficiency and cellular response to paclitaxel in prostate cancer cells. Prostate 2001;48:254–64.
[14] Stewart ZA, Leach SD, Pietenpol JA. p21(Waf1/Cip1) inhibition of cyclin E/Cdk2 activity prevents endoreduplication after mitotic spindle disruption. Mol Cell Biol 1999;19:205–15.
[15] Thannickal VJ, Fanburg BL. Reactive oxygen species in cell signaling. Am J Physiol Lung Cell Mol Physiol 2000;279:L1005–28.
[16] Liu B, Cheng Y, Bian HJ, Bao JK. Molecular mechanisms of Polygonatum cyrtonema lectin-induced apoptosis and autophagy in cancer cells. Autophagy 2009;5:253–5.
[17] Ahmed K, Matsuya Y, Nemoto H, Zaidi SF, Sugiyama T, Yoshihisa Y, et al. Mechanism of apoptosis induced by a newly synthesized derivative of macrosphelides with a thiazole side chain. Chem Biol Interact 2009;177:218–26.
[18] Han YH, Kim SW, Kim SH, Kim SZ, Park WH. 2,4-Dinitrophenol induces G1 phase arrest and apoptosis in human pulmonary adenocarcinoma Calu-6 cells. Toxicol In Vitro 2008;22:659–70.
[19] Tayama S, Nakagawa Y. Effect of scavengers of active oxygen species on cell damage caused in CHO-K1 cells by phenylhydroquinone, an o-phenylphenol metabolite. Mutat Res 1994;324:121–31.
[20] Huang DP, Ho JH, Poon YF, Chew EC, Saw D, Lui M, et al. Establishment of a cell line (NPC/HK1) from a differentiated squamous carcinoma of the nasopharynx. Int J Cancer 1980;26:127–32.
[21] Lo AK, Lo KW, Tsao SW, Wong HL, Hui JW, To KF, et al. Epstein-Barr virus infection alters cellular signal cascades in human nasopharyngeal epithelial cells. Neoplasia 2006;8:173–80.
[22] Cheung ST, Huang DP, Hui AB, Lo KW, Ko CW, Tsang YS, et al. Nasopharyngeal carcinoma cell line (C666-1) consistently harbouring Epstein-Barr virus. Int J Cancer 1999;83:121–6.
[23] Cheng Y, Poulos NE, Lung ML, Hampton G, Ou B, Lerman MI, et al. Functional evidence for a nasopharyngeal carcinoma tumor suppressor gene that maps at chromosome 3p21.3. Proc Natl Acad Sci USA 1998;95:3042–7.
[24] Pelicano H, Carney D, Huang P. ROS stress in cancer cells and therapeutic implications. Drug Resist Updat 2004;7:97–110.
[25] Chambard JC, Lefloch R, Pouyssegur J, Lenormand P. ERK implication in cell cycle regulation. Biochim Biophys Acta 2007;1773:1299–310.
[26] Fukui M, Zhu BT. Mechanism of 2-methoxyestradiol-induced apoptosis and growth arrest in human breast cancer cells. Mol Carcinog 2009;48:66–78.
[27] Qadan LR, Perez-Stable CM, Anderson C, D'Ippolito G, Herron A, Howard GA, et al. 2-Methoxyestradiol induces G2/M arrest and apoptosis in prostate cancer. Biochem Biophys Res Commun 2001;285:1259–66.
[28] Zhou NN, Zhu XF, Zhou JM, Li MZ, Zhang XS, Huang P, et al. 2-Methoxyestradiol induces cell cycle arrest and apoptosis of nasopharyngeal carcinoma cells. Acta Pharmacol Sin 2004;25:1515–20.
[29] Kijima T, Kinukawa N, Gooding WE, Uno M. Association of Epstein-Barr virus with tumor cell proliferation: clinical implication in nasopharyngeal carcinoma. Int J Oncol 2001;18:479–85.

[30] Edgar BA, Orr-Weaver TL. Endoreplication cell cycles: more for less. Cell 2001;105:297–306.
[31] Damiens E, Baratte B, Marie D, Eisenbrand G, Meijer L. Anti-mitotic properties of indirubin-3′-monoxime, a CDK/GSK-3 inhibitor: induction of endoreplication following prophase arrest. Oncogene 2001;20:3786–97.
[32] Gui Y, Zheng XL. 2-methoxyestradiol induces cell cycle arrest and mitotic cell apoptosis in human vascular smooth muscle cells. Hypertension 2006; 47:271–80.
[33] Gui Y, Yin H, He JY, Yang SH, Walsh MP, Zheng XL. Endoreduplication of human smooth muscle cells induced by 2-methoxyestradiol: a role for cyclin-dependent kinase 2. Am J Physiol Heart Circ Physiol 2007;292:H1313–20.
[34] Puig PE, Guilly MN, Bouchot A, Droin N, Cathelin D, Bouyer F, et al. Tumor cells can escape DNA-damaging cisplatin through DNA endoreduplication and reversible polyploidy. Cell Biol Int 2008;32:1031–43.
[35] Zhang W, Liu HT. MAPK signal pathways in the regulation of cell proliferation in mammalian cells. Cell Res 2002;12:9–18.
[36] Pearson G, Robinson F, Beers GT, Xu BE, Karandikar M, Berman K, et al. Mitogen-activated protein (MAP) kinase pathways: regulation and physiological functions. Endocr Rev 2001;22:153–83.
[37] Moon DO, Kim MO, Kang SH, Lee KJ, Heo MS, Choi KS, et al. Induction of G2/M arrest, endoreduplication, and apoptosis by actin depolymerization agent pextenotoxin-2 in human leukemia cells, involving activation of ERK and JNK. Biochem Pharmacol 2008;76:312–21.
[38] Wang M, Atayar C, Rosati S, Bosga-Bouwer A, Kluin P, Visser L. JNK is constitutively active in mantle cell lymphoma: cell cycle deregulation and polyploidy by JNK inhibitor SP600125. J Pathol 2009;218:95–103.
[39] Lee CF, Liu CY, Hsieh RH, Wei YH. Oxidative stress-induced depolymerization of microtubules and alteration of mitochondrial mass in human cells. Ann N Y Acad Sci 2005;1042:246–54.
[40] Rajkumar SV, Richardson PG, Lacy MQ, Dispenzieri A, Greipp PR, Witzig TE, et al. Novel therapy with 2-methoxyestradiol for the treatment of relapsed and plateau phase multiple myeloma. Clin Cancer Res 2007;13:6162–7.
[41] Tevaarwerk AJ, Holen KD, Alberti DB, Sidor C, Arnott J, Quon C, et al. Phase I trial of 2-methoxyestradiol nanocrystal dispersion in advanced solid malignancies. Clin Cancer Res 2009;15:1460–5.
[42] LaVallee TM, Burke PA, Swartz GM, Hamel E, Agoston GE, Shah J, et al. Significant antitumor activity in vivo following treatment with the microtubule agent ENMD-1198. Mol Cancer Ther 2008;7:1472–82.